PHYSICAL REVIEW B **92**, 125422 (2015)

Impurity-induced quantum phase transitions and magnetic order in conventional superconductors: Competition between bound and quasiparticle states

Silas Hoffman,[1] Jelena Klinovaja,[1] Tobias Meng,[1,2] and Daniel Loss[1]
[1] *Department of Physics, University of Basel, Klingelbergstrasse 82, CH-4056 Basel, Switzerland*
[2] *Institut für Theoretische Physik, Technische Universität Dresden, 01062 Dresden, Germany*
(Received 2 April 2015; published 16 September 2015)

We theoretically study bound states generated by magnetic impurities within conventional s-wave superconductors, both analytically and numerically. In determining the effect of the hybridization of two such bound states on the energy spectrum as a function of magnetic exchange coupling, relative angle of magnetization, and distance between impurities, we find that quantum phase transitions can be modulated by each of these parameters. Accompanying such transitions, there is a change in the preferred spin configuration of the impurities. Although the interaction between the impurity spins is overwhelmingly dominated by the quasiparticle contribution, the ground state of the system is determined by the bound-state energies. Self-consistently calculating the superconducting order parameter, we find a discontinuity when the system undergoes a quantum phase transition as indicated by the bound-state energies.

DOI: 10.1103/PhysRevB.92.125422 PACS number(s): 75.30.Hx, 74.25.Ha, 75.30.Kz, 73.20.Hb

I. INTRODUCTION

In a conventional s-wave superconductor, quasiparticle excitation energies are separated from the chemical potential due to the formation of the superconducting gap. When magnetic impurities are present, the exchange interaction can induce a bound state within the gap known as a Yu-Shiba-Rusinov (YSR) state [1], which has been studied in detail both experimentally and theoretically [2–15]. Recently, these states have attracted much attention in the context of magnetic impurity chains in which, when sufficiently close together, individual YSR states can hybridize with adjacent bound states to form a band within the superconducting gap that can host Majorana fermions at its ends [16–27].

Two magnetic impurities interacting via quasiparticles are well described by the Ruderman-Kittel-Kasuya-Yosida (RKKY) interaction [28–32] when the exchange interaction between the impurity and quasiparticles is much smaller than the Fermi energy. This results in a noncollinear orientation between the impurities in three-dimensional superconductors [33,34]. Although for many parameters the contribution to the interimpurity exchange mediated by the overlap of YSR states is much smaller than that of the quasiparticles [34–36], it has been shown that resonant YSR bound states can dominate the exchange interaction and induce an antiferromagnetic alignment of the impurities [11]. However, for the experimentally relevant limit [24] when the exchange interaction is of the order of the Fermi energy, a theoretical understanding of the interaction between magnetic impurities including (1) the quasiparticle contribution and (2) a self-consistent local reduction of the gap is missing from the literature.

In this manuscript, we determine the interaction between two magnetic impurities for arbitrary angles between their spins wherein the strength of the exchange interaction is unrestricted and, in general, unequal at the sites of the impurities. In the following section, we detail the Hamiltonian used to study the impurity interactions analytically and define the ground-state energy, which determines the energetically favored magnetic configuration, of the superconductor-impurity system. In Sec. III, by analytically calculating the bound-state energy spectrum, we find that a quantum phase transition (QPT) [4–9,14] can be tuned by changing the distance between and relative magnetic orientation of the impurities. In Sec. IV, we, numerically, include the bulk contribution to the exchange interaction which we find quantitatively dominates over the YSR contribution for many parameters [11,34–36]. Further, carrying out self-consistently calculations, we find a discontinuity in the superconducting order parameter when the system undergoes such a QPT as indicated by the bound-state energies. This, in turn, gives rise to magnetic metastable states, in addition to the lowest-energy magnetic configuration, for a sufficiently large exchange interaction. In the final section, we summarize our results.

II. MODEL

We consider two magnetic impurities embedded in a bulk s-wave superconductor, see Fig. 1. The quasiparticles interact with the impurity spins through the exchange interaction that produces a local effective magnetic field. The corresponding Bogoliubov-de Gennes (BdG) Hamiltonian density is given by

$$H = \xi_{\mathbf{p}}\tau_z + \Delta(\mathbf{r})\tau_x - \sum_{i=1,2} J_i \mathbf{S}_i \cdot \boldsymbol{\sigma}\,\delta(\mathbf{r}_i - \mathbf{r})\,, \qquad (1)$$

where $\xi_{\mathbf{p}}$ is the dispersion of the quasiparticles with momentum $\mathbf{p}$ in the normal metal phase and $\Delta(\mathbf{r})$ is the local superconducting pairing strength. The Pauli matrices $\boldsymbol{\tau}$ ($\boldsymbol{\sigma}$) act in Nambu (spin) space. The exchange coupling strength J_i of the spin impurity at $\mathbf{r}_i$ can be positive or negative corresponding to ferro- or antiferromagnetic interactions with quasiparticles, respectively. Here, we focus on $J_i > 0$ without loss of generality. We assume that $\mathbf{S}_i$ are the classical spin vectors of the impurity at $\mathbf{r}_i$, and θ is the angle between them. The magnitude of the spins, $S_i = |\mathbf{S}_i|$, are much larger than $\hbar$ so that quantum mechanical spin fluctuations, e.g., the Kondo effect, are negligible. In the following analytics, we assume that $\Delta(\mathbf{r}) = \Delta_0$ is spatially uniform and neglect its suppression due to the impurities [6,37], which we account for self-consistently in the numerics following earlier work [4–9,14].

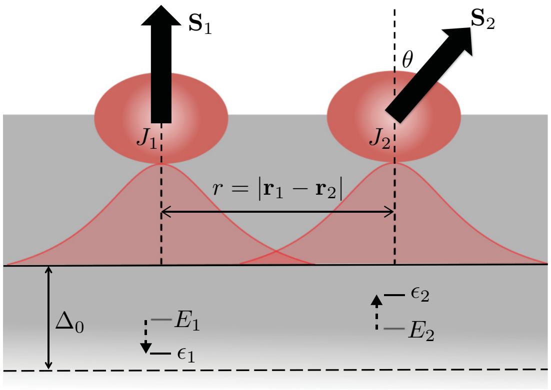

FIG. 1. (Color online) Our setup of two magnetic impurities at $\mathbf{r}_1$ and $\mathbf{r}_2$ in an s-wave superconductor with classical spins $\mathbf{S}_1$ and $\mathbf{S}_2$, respectively, oriented at a relative angle θ. As a result of the magnetic exchange couplings, J_1 and J_2, YSR bound states form within the bulk gap Δ_0. When the distance between the impurities, r, is larger than the coherence length of the superconductor the energies are E_1 and E_2 but get changed to ϵ_1 and ϵ_2 as r decreases and the bound states hybridize with each other.

To determine the energy of the bound states $\epsilon_{1,2}$ and $-\epsilon_{1,2}$, where the latter is due to the particle-hole symmetry of Eq. (1), we apply a straightforward calculation along the lines of Ref. [21] and obtain a coupled set of secular equations for the BdG four-component spinors $\psi(\mathbf{r})$ at $\mathbf{r}_1$ and $\mathbf{r}_2$,

$$\begin{aligned}\psi(\mathbf{r}_1) &= \hat{J}_1 \mathbf{s}_1 \cdot \boldsymbol{\sigma}\, \psi(\mathbf{r}_1) + \hat{\Gamma}_2 \mathbf{s}_2 \cdot \boldsymbol{\sigma}\, \psi(\mathbf{r}_2)\,,\\ \psi(\mathbf{r}_2) &= \hat{J}_2 \mathbf{s}_2 \cdot \boldsymbol{\sigma}\, \psi(\mathbf{r}_2) + \hat{\Gamma}_1 \mathbf{s}_1 \cdot \boldsymbol{\sigma}\, \psi(\mathbf{r}_1)\,,\end{aligned} \tag{2}$$

where $\mathbf{s}_i = \mathbf{S}_i/S_i$ and

$$\hat{J}_i = \frac{\alpha_i(\epsilon + \tau_x \Delta_0)}{\sqrt{\Delta_0^2 - \epsilon^2}}, \tag{3}$$

$$\hat{\Gamma}_i = \alpha_i \left(\frac{(\epsilon + \tau_x \Delta_0) \sin k_F r}{\sqrt{\Delta_0^2 - \epsilon^2}} + \tau_z \right) \frac{e^{-r/\xi_\epsilon}}{k_F r} \tag{4}$$

for $i = 1,2$. Here, $\alpha_i = \nu_0 \pi J_i S_i$, where ν_0 is the density of states evaluated at the Fermi energy, $r = |\mathbf{r}_1 - \mathbf{r}_2|$ is the distance between the impurities, k_F (v_F) is the Fermi wave vector (Fermi velocity) and $\xi_\epsilon = v_F/\sqrt{\Delta_0^2 - \epsilon^2}$.

When the distance between impurities is much greater than the superconducting coherence length, $r \gg \xi_0$, the impurities effectively decouple, $\hat{\Gamma}_i \to 0$, and one finds that Eq. (2) furnishes solutions of unhybridized YSR bound states at $\mathbf{r}_1$ and $\mathbf{r}_2$ with energies $\pm E_i = \pm\Delta_0(1 - \alpha_i^2)/(1 + \alpha_i^2)$ [1,21]. In this limit, for sufficiently large exchange interaction, $J_i > 1/\nu_0 \pi S_i$, the bound-state energy goes below the chemical potential and the system undergoes a QPT wherein the parity of the ground changes [4–6,38]. In order to determine the energies of the hybridized bound states analytically from Eq. (2), we focus on distances between impurities much smaller than the coherence length, $r \ll \xi_0$, so that $e^{-r/\xi_\epsilon} \approx 1$ so that the hybridization is determined to leading order by $1/k_F r$.

To determine the total ground-state energy of our system, we formally diagonalize the Hamiltonian and use a variational wave function as an ansatz for the ground state by extending the variational wave function from one impurity [6] to two impurities. For sufficiently weak coupling, in both the exchange interaction (α_1, $\alpha_2 \lesssim 1$) and the bound-state hybridization ($k_F r \gtrsim 1$), the ground state is given by the BCS-like wave function $|\Psi_0\rangle \sim \prod_{n>0}(u_n + v_n \psi_n^\dagger \psi_{-n}^\dagger |0\rangle$, where ψ_n furnish a basis for the BdG Hamiltonian in the presence of the impurities for a given magnetic alignment and u_n and v_n are the Bogoliubov coherence factors. The quasiparticle operators γ_n are defined as $\gamma_1 = u_1\psi_1 - v_1\psi_{-1}^\dagger$, $\gamma_{-1}^\dagger = u_1\psi_{-1} + v_1\psi_1^\dagger$, $\gamma_1^\dagger = u_1\psi_1^\dagger - v_1\psi_{-1}$, and similarly for $n > 1$, so that $\gamma_n|\Psi_0\rangle = 0$ for all n. Let $n = 1$ correspond to the lower-energy bound state and $n = 2$ to the higher one while $-n$ corresponds to a state with reversed spin. When the lower-energy bound state is occupied, the wave function is given by $|\Psi_1\rangle \sim \gamma_1^\dagger|\Psi_0\rangle = \psi_1^\dagger \prod_{n>1}(u_n + v_n\psi_n^\dagger\psi_{-n}^\dagger)|0\rangle$. When both states are occupied, the wave function is $|\Psi_{1,2}\rangle \sim \gamma_2^\dagger|\Psi_1\rangle = \gamma_2^\dagger\gamma_1^\dagger|\Psi_0\rangle = \psi_2^\dagger\psi_1^\dagger \prod_{n>2}(u_n + v_n\psi_n^\dagger\psi_{-n}^\dagger)|0\rangle$. As the hybridization between the bound states or the exchange coupling increases, the lower energy state becomes occupied and the ground state is $|\Psi_1\rangle$. When both states are below the chemical potential, the ground state then becomes $|\Psi_{1,2}\rangle$. To determine the total energy of the system, one can diagonalize the Hamiltonian using a Bogoliubov transformation, $H = \sum_n \epsilon_n(\theta)(\gamma_n^\dagger\gamma_n - \frac{1}{2})$ [11], where ϵ_n is the energy of state n. The ground-state energies are therefore [6,11]

$$\mathcal{E}_{gr}(\theta) = -\frac{1}{2}\sum_n |\epsilon_n(\theta)|. \tag{5}$$

In the following analytics, we focus on the bound states and therefore only include the YSR contribution to the summation in Eq. (5): $\mathcal{E}(\theta) = -(|\epsilon_1(\theta)| + |\epsilon_2(\theta)|)/2$.

III. HYBRIDIZATION BETWEEN BOUND STATES

For the moment, we consider the case of weak hybridization ($k_F r \gg E_i/\Delta_0$) for YSR states sufficiently far away from the chemical potential, so that the occupation of the bound states, and thus the ground state, is fixed by α_i. That is, when $\alpha_i < 1$ ($\alpha_i > 1$), the energy is above (below) the chemical potential. Calculating the full analytic solution and then expanding to second order in $1/k_F r$, which is valid when $|1 - \alpha_i|k_F r \gg 1$ and $|\alpha_1 - \alpha_2|k_F r \gg 1$ [39], the spectrum has two solutions of the form

$$\epsilon_n(\theta) \approx E_n + \Delta_0(A_n + B_n \cos\theta)/(k_F r)^2, \tag{6}$$

where the coefficients A_n and B_n are functions of α_1, α_2, and $k_F r$ (Appendix). The bound-state energy is extremized when either $\theta = 0$ or π, i.e., the ground state of impurities is collinear. When $\epsilon_1\epsilon_2 > 0$, $\mathcal{E}(\pi)$ is always smaller than $\mathcal{E}(0)$ [11] and therefore the ground state is antiferromagnetic. When $\epsilon_1\epsilon_2 < 0$, $\mathcal{E}(\pi) > \mathcal{E}(0)$ and a ferromagnetic orientation is favored. See Appendix for a detailed derivation.

Although strong hybridization between impurities cannot be addressed perturbatively, in the symmetric case of equal exchange coupling, i.e., $\alpha_1 = \alpha_2 \equiv \alpha$, Eq. (2) can be solved directly. Because the analytic solution for arbitrary θ is too involved, we focus here on collinear alignments. In the ferromagnetic configuration, the bound-state energy levels are given by

$$\epsilon_\pm^F \equiv \epsilon_{1,2}(0) = -\Delta_0(a \pm b)/\sqrt{(a \pm b)^2 + c^2}\,, \tag{7}$$

where

$$\begin{aligned} a &= \alpha\left\{\alpha^2\left[1 + \left(\frac{1}{k_F r}\right)^2 \cos 2k_F r\right] - 1\right\},\\ b &= \alpha \frac{\sin k_F r}{k_F r}\left\{\alpha^2\left[\left(\frac{1}{k_F r}\right)^2 - 1\right] - 1\right\},\\ c &= \alpha^2\left[2 + \left(\frac{1}{k_F r}\right)^2 (\cos 2k_F r - 1)\right]. \end{aligned} \tag{8}$$

The initially twofold degenerate energy levels of the bound states are both split due to hybridization and shifted due to the effective Zeeman splitting at both $\mathbf{r}_1$ and $\mathbf{r}_2$.

In the antiferromagnetic configuration, the energy level stays twofold degenerate [8] and is given by

$$\epsilon^A \equiv \epsilon_{1,2}(\pi) = \Delta_0 \sqrt{\frac{(1-\alpha^2)^2 + 2(\alpha/k_F r)^2 + d}{(1+\alpha^2)^2 + 2(\alpha/k_F r)^2 \cos 2k_F r + d}}\,, \tag{9}$$

where

$$d = \alpha^4 (1 + 2\cos 2k_F r)\left(\frac{1}{k_F r}\right)^4. \tag{10}$$

In this case, although there is no hybridization of the bound states, the energies of the localized YSR states are shifted away from the single impurity solutions due to the effective Zeeman field of the second impurity.

To determine the favored collinear orientation of the magnetic impurities, it is convenient to define $\delta\mathcal{E} \equiv \mathcal{E}(0) - \mathcal{E}(\pi) = -(|\epsilon_F^+| + |\epsilon_F^-| - 2|\epsilon^A|)/2$, the difference between the ground-state energies in the collinear configurations, so that when $\delta\mathcal{E} > 0$ the system prefers an antiferromagnetic orientation while when $\delta\mathcal{E} < 0$ the system prefers an ferromagnetic orientation of the impurities.

When $\alpha = 0.5$ [Fig. 2 (upper panel)], all the electronlike energies in either configuration defined by Eqs. (7) and (9) are greater than zero, in the displayed range, $k_F r \geqslant 1$. Furthermore, $\delta\mathcal{E} > 0$ and therefore the exchange interaction between impurities is antiferromagnetic, in agreement with the weak coupling limit. If the impurity levels are close to the chemical potential, e.g., $\alpha = 0.9$ [Fig. 2 (lower panel)], the ground state of the system depends on the distance between the impurities. When r is sufficiently large, so that the condition for weak hybridization is met, $\epsilon_\pm^F, \epsilon^A, \delta\mathcal{E} > 0$, and the preferred ordering is antiferromagnetic. When $k_F r \approx 8$, ϵ_F^- goes below the chemical potential. Near this value of $k_F r$, $\delta\mathcal{E}$ becomes negative and therefore the preferred magnetic ground state is ferromagnetic rather than antiferromagnetic. As the distance between the impurities decreases further, the bound-state energies oscillate about the chemical potential as a function of r, thereby changing the ground state of the system. As a result, $\delta\mathcal{E}$ also oscillates around zero implying a change between ferromagnetic and antiferromagnetic configurations.

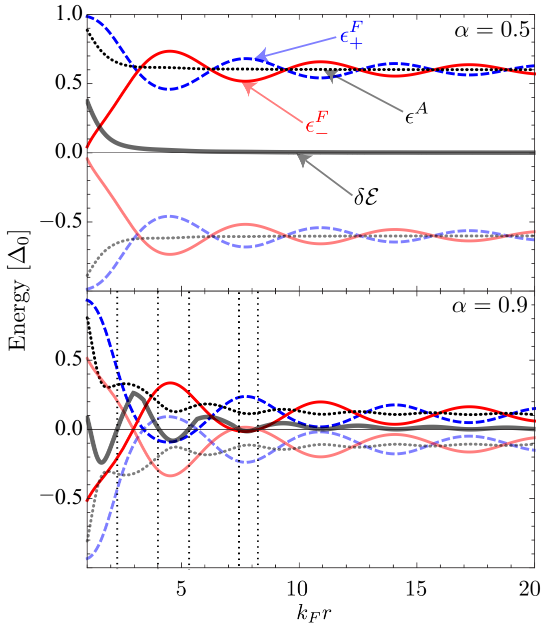

FIG. 2. (Color online) Energy of the YSR bound states for the identical magnetic impurities oriented ferromagnetically (solid and dashed) and antiferromagnetically (dotted) as well as the energy difference $\delta\mathcal{E}$ (thick solid lines) as a function of the distance r between impurities. When $\alpha = 0.5$ (top panel), the system remains antiferromagnetic ($\delta\mathcal{E} > 0$), while for $\alpha = 0.9$ (lower panel), the magnetic configuration oscillates between being antiferromagnetic and ferromagnetic. For convenience, these two configurations are separated by the vertical dotted lines.

As we have seen, for some values of r ($|E_i|/\Delta_0 \lesssim k_F r$), the bound-state energies are on opposite sides of the chemical potential in the ferromagnetic configuration due to hybridization, while in the antiferromagnetic configuration the energies are always degenerate. Therefore, quite remarkably, one may drive a QPT by changing the relative angle of the impurities. To illustrate this, we exactly solve Eq. (2) for generally α_1, α_2, r, and θ. The solution, although straightforward, is physically opaque. We therefore plot ϵ_1, ϵ_2, and $\mathcal{E}$ as a function of θ, fixing $k_F r = 1$, $\alpha_1 = 0.5$, and $\alpha_2 = 1$ in Fig. 3. At $\theta \approx \pi/2$,

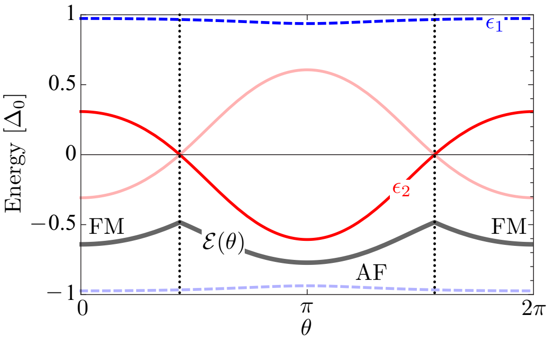

FIG. 3. (Color online) The energy of the bound states (ϵ_1, ϵ_2) and the total YSR state energy [$\mathcal{E}(\theta)$] as a function of relative angle θ for $k_F r = 1$, $\alpha_1 = 0.5$, and $\alpha_2 = 1$. The change of quantum ground state at $\theta \approx \pm\pi/2$ is indicated by vertical dotted lines.

ϵ_2 goes from positive to negative, i.e., one of the YSR bound states passes through the chemical potential, signaling a QPT. Accompanying this change in the ground state of the system is a kink in $\mathcal{E}$. As a result, although the energy is minimized in the antiferromagnetic configuration, $\theta = \pi$, there is a local minimum in energy when the impurities are oriented ferromagnetically. Therefore, while the parameters chosen favor an antiferromagnetic configuration as an *absolute* ground state, they additionally support a *metastable* ferromagnetic configuration [40].

IV. BULK CONTRIBUTION TO TOTAL ENERGY

To address the contributions coming from the bulk, we follow earlier work [4–9,14] and numerically study a two-dimensional system with two magnetic impurities, determining self-consistently the renormalization of the gap which cannot be addressed analytically [14,37] for large exchange interaction. We use the tight-binding Hamiltonian

$$\begin{aligned}\bar{H} = &-t\sum_{\langle i,i'\rangle}\sum_{\sigma=\pm 1} c^\dagger_{i\sigma}c_{i'\sigma} + \sum_i (\Delta_i c_{i1}c_{i\bar{1}} + \text{H.c.})\\ &+\sum_i\sum_{\sigma=\pm 1}([\mu - 4t + (\delta_{i1}+\delta_{i2})\bar{J}_i\sigma\cos\theta_i]c^\dagger_{i\sigma}c_{i\sigma}\\ &+(\delta_{i1}+\delta_{i2})\bar{J}_i\sin\theta_i\, c^\dagger_{i\sigma}c_{i\bar{\sigma}}),\end{aligned} \tag{11}$$

where $c_{i\sigma}$ is the annihilation operator acting on an electron with spin σ at lattice site i, and the first sum runs over neighboring sites i and i' located in a two-dimensional square lattice of size $N_x \times N_y$ with lattice constant a. The chemical potential μ is taken from the bottom of the energy band, and the local order parameter Δ_i is determined self-consistently in an iterative fashion for fixed values of the exchange coupling $\bar{J}_i$ at site i starting from the uniform superconducting order parameter Δ_0. To compare to the analytics, we consider two impurities located at $i = 1$ and $i = 2$ (which are not necessarily adjacent) with equal exchange coupling, $\bar{J} = \bar{J}_1 = \bar{J}_2$, and fixing the difference in magnetic orientation to be θ, mirroring the schematics of Fig. 1. After numerically diagonalizing Eq. (11), we find two types of energies in the spectrum: in-gap YSR bound states, analogous to those found analytically in the previous section, and supragap energies corresponding to the quasiparticle spectrum. In order to directly compare with the results of the previous section, we calculate $\mathcal{E}$ by summing only the energies of the in gap states. However, to calculate the full ground state including both quasiparticle and YSR energies, we use $\mathcal{E}_{gr}$ as define by Eq. (5), summing all energies below the chemical potential.

Focusing first on the YSR states, we plot $\delta\mathcal{E}$ as a function of r in Fig. 4. When $\bar{J}/t = 1$ [Fig. 4(a)], $\delta\mathcal{E}$ is positive for nearly all values of r indicating an antiferromagnetic configuration is preferred. However, for $\bar{J}/t = 2.5$ [Fig. 4(b)], $\delta\mathcal{E}$ oscillates between positive and negative values. Although in the numerics we have taken into account the position-dependent renormalization of the gap, the results are in good agreement with the analytics of the previous section (Fig. 2). When the exchange interaction strength is further increased to $\bar{J}/t = 4$ [Fig. 4(c)], the difference between the YSR state energies in the collinear magnetic configurations is positive for nearly all values of r, indicating that the antiferromagnetic orientation is preferred, again in good agreement with the analytics.

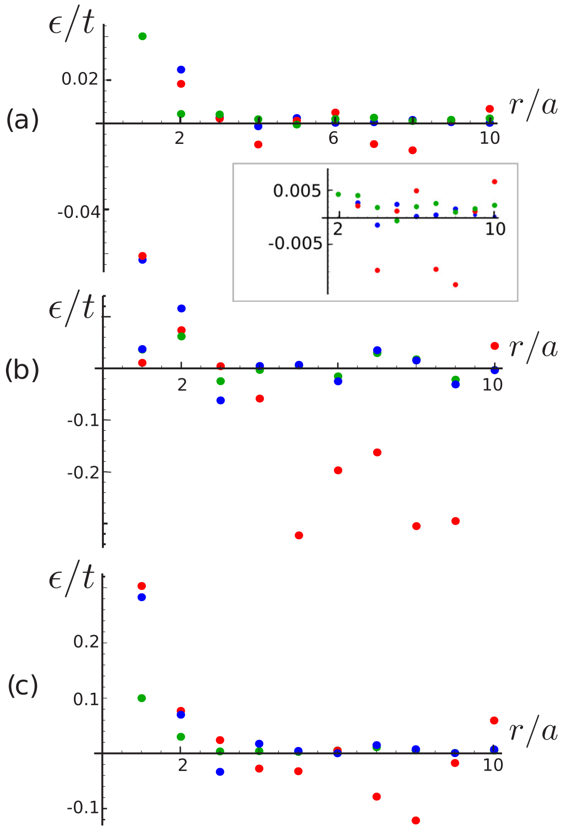

FIG. 4. (Color online) The difference in the energy $\delta\mathcal{E}_{gr}$ between ferro- and antiferromagnetic configurations of the system consisting of two identical impurities of coupling strength $\bar{J}$ as a function of the distance between impurities, r/a, for (a) $\bar{J}/t = 1$ and (b) $\bar{J}/t = 2.5$ found self-consistently (red dots) and not self-consistently (blue dots), respectively. Inset: enlarged area of (a) for large distances. The difference in the energy $\delta\mathcal{E}$ between ferro- and antiferromagnetic configurations including only the YSR bound state (green dots) is found self-consistently. The parameters used are $N_x \times N_y = 33 \times 25$, $\mu/t = 1$, and $\Delta_0/t = 0.1$.

In order to distinguish the effect of gap renormalization from the quasiparticle contribution, we first plot $\delta\mathcal{E}_{gr} = \mathcal{E}(0) - \mathcal{E}(\pi)$, *without* self-consistent renormalization of the gap, i.e., $\Delta_i = \Delta_0$, as a function of r in Fig. 4. Interestingly, $\delta\mathcal{E}_{gr}$ is changed only slightly for all values of $\bar{J}$, keeping the $\delta\mathcal{E}_{gr}$ at the same order of magnitude as $\delta\mathcal{E}$. Upon including renormalization of the gap, $\delta\mathcal{E}_{gr}$ is increased drastically and the ground-state magnetic orientation becomes very sensitive to the distance between the impurities. Although the exact functional dependence is unclear, this emphasizes the importance of a self-consistent renormalization of the gap when calculating the energies of such a system, particularly when close to the QPT.

Fixing the distance between the impurities to $r/a = 6$, we calculate $\mathcal{E}_{gr}$ and $\mathcal{E}$ as a function of relative angle and observe that away from the phase transition, $\mathcal{E}_{gr}$ and $\mathcal{E}$ change monotonically for $\theta \in [0,\pi]$, and, thus, the ground state is either ferromagnetic or antiferromagnetic, consistent

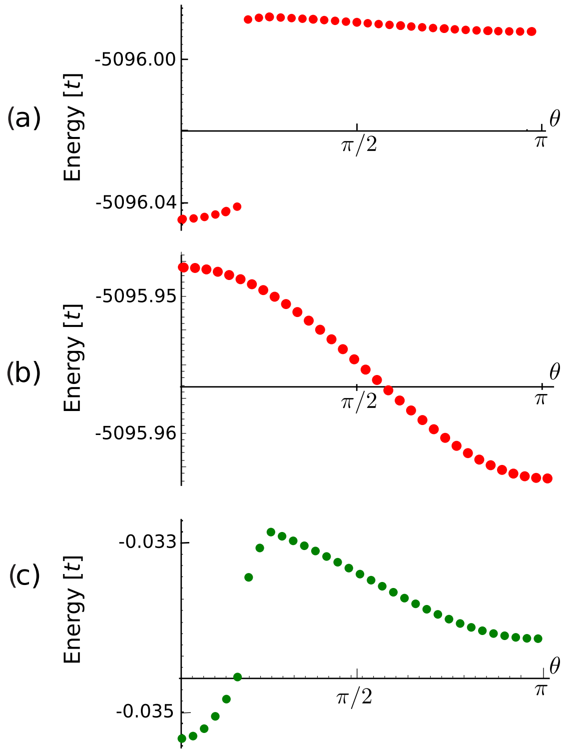

FIG. 5. (Color online) The total energy of the ground state for two identical impurities ($\bar{J} = \bar{J}_1 = \bar{J}_2$) as a function of the angle θ between magnetic moments found numerically for (a) $\bar{J}/t = 2.17$ (ferromagnetic ordering) and (b) $\bar{J}/t = 2$ (antiferromagnetic ordering) at the distance $r/a = 6$. We additionally plot (c) $\mathcal{E}(\theta)$ for $\bar{J}/t = 2.17$ also at $r/a = 6$. Other parameters are the same as in Fig. 4.

with the analytical results. For instance, when $\bar{J}/t = 2$, before the QPT, the system prefers an antiferromagnetic configuration [Fig. 5(b)], similar to the analytics. Close to the phase transition, the bound-state energies cross the chemical potential as a function of θ. As a result, there is a jump in the ground-state energy at the QPT so that $\mathcal{E}_{gr}(\theta)$ is a nonmonotonic function of θ in the range $[0,\pi]$. As such, when the ground state is ferromagnetic (antiferromagnetic), there is an additional metastable antiferromagnetic (ferromagnetic) state. For instance, when $\bar{J}/t = 2.17$ [Fig. 5(a)], the ground state is ferromagnetic but there is an additional metastable antiferromagnetic configuration. Considering only the YSR contributions to the energy, we plot $\mathcal{E}(\theta)$ [Fig. 5(c)] and find a ground state and a metastable state at the collinear configurations of the magnetizations, in agreement with the analytics. However, because of the self-consistent renormalization of the gap, there is a jump in $\mathcal{E}$ at $\theta \approx \pi/6$ where the QPT occurs. We note that the jump in $\mathcal{E}$ is several orders of magnitude smaller than $\mathcal{E}_{gr}$. Thus the magnitude of the interaction is dominated by the quasiparticle contribution to the ground-state energy. However, the QPT is determined by the position of the bound states with respect to the chemical potential which, in turn, introduces a metastable state.

V. CONCLUSIONS

We have studied how the orientation of two spin impurities coupled via overlap of the YSR bound states induced by them depends on the distance between impurities and the strength of the exchange interaction. We have also demonstrated that a QPT can be controlled by changing relative magnetic orientation. Generally, the bulk contribution to the total ground-state energy dominates over the bound-state contribution, especially if the superconducting order parameter is determined self-consistently. The proposed effects could be measured with STM [46] or NV-center [47,48] techniques.

ACKNOWLEDGMENTS

We acknowledge support from the Swiss NSF, NCCR QSIT, and the DFG through GRK 1621 and SFB 1143.

APPENDIX: HYBRIDIZATION IN WEAK COUPLING LIMIT

To obtain the energetically favorable magnetic orientation in the weak coupling limit, we solve Eq. (2) of the main text for the in-gap energies and expand to second order in $1/k_F r$. We find the bound-state energies are

$$\epsilon_n(\theta) \approx E_n + \Delta_0(A_n + B_n \cos\theta)\left(\frac{1}{k_F r}\right)^2, \tag{A1}$$

with

$$\begin{aligned}
A_1 &= \frac{-2\alpha_1^2\alpha_2^2(1-\alpha_2^4) + 2\alpha_1\alpha_2(1+\alpha_1^4 - 2\alpha_1^2\alpha_2^2)\cos 2k_F r}{(1+\alpha_1^2)^2[\alpha_2^2(1+\alpha_1^4) - \alpha_1^2(1+\alpha_2^4)]},\\
B_1 &= \frac{-2\alpha_2\alpha_1^3(1+\alpha_1^2-\alpha_2^2-\alpha_1^2\alpha_2^2)(1-\alpha_2^2) + 2\alpha_2\alpha_1^3(1-\alpha_1^2+\alpha_2^2-\alpha_1^2\alpha_2^2)\cos 2k_F r}{(1+\alpha_1^2)^2[\alpha_2^2(1+\alpha_1^4) - \alpha_1^2(1+\alpha_2^4)]},\\
A_2 &= \frac{2\alpha_1^2\alpha_2^2(1-\alpha_1^4) - 2\alpha_1\alpha_2(1+\alpha_2^4 - 2\alpha_1^2\alpha_2^2)\cos 2k_F r}{(1+\alpha_2^2)^2[\alpha_2^2(1+\alpha_1^4) - \alpha_1^2(1+\alpha_2^4)]},\\
B_2 &= \frac{2\alpha_1\alpha_2^3(1-\alpha_1^2+\alpha_2^2-\alpha_1^2\alpha_2^2)(1-\alpha_1^2) - 2\alpha_1\alpha_2^3(1+\alpha_1^2-\alpha_2^2-\alpha_1^2\alpha_2^2)\cos 2k_F r}{(1+\alpha_2^2)^2[\alpha_2^2(1+\alpha_1^4) - \alpha_1^2(1+\alpha_2^4)]}.
\end{aligned} \tag{A2}$$

We consider three cases: when the bare energies are both above the chemical potential, both below the chemical potential, or on opposite sides of the chemical potential. The total energy of the system, according to Eq. (5) of the main text, is given by

$$\mathcal{E}(\theta) = \begin{cases} -[\epsilon_1(\theta) + \epsilon_2(\theta)]/2\,, & \epsilon_1 > 0, \epsilon_2 > 0 \\ [\epsilon_2(\theta) - \epsilon_1(\theta)]/2\,, & \epsilon_1 < 0, \epsilon_2 > 0\,. \\ [\epsilon_1(\theta) + \epsilon_2(\theta)]/2\,, & \epsilon_1 < 0, \epsilon_2 < 0 \end{cases} \tag{A3}$$

In all cases, the total energy is extremized when $\theta = 0,\pi$, and for no intermediate values of θ. To determine the energetically favored magnetic configuration, we calculate $\delta\mathcal{E} \equiv \mathcal{E}(0) - \mathcal{E}(\pi)$. When both energies are above the chemical potential,

$$\begin{aligned}
\frac{\delta\mathcal{E}}{\Delta_0} &= 2\alpha_1\alpha_2\left(\frac{1}{k_F r}\right)^2\left[\frac{1+\alpha_1^2+\alpha_2^2+2\alpha_1^2\alpha_2^2+\alpha_1^4\alpha_2^2+\alpha_1^2\alpha_1^4+\alpha_1^4\alpha_2^4}{\left(1+\alpha_1^2\right)^2\left(1+\alpha_2^2\right)^2\left(1-\alpha_1^2\alpha_2^2\right)}\right. \\
&\quad \left. -\frac{1-\alpha_1^2-\alpha_2^2-6\alpha_1^2\alpha_2^2-\alpha_1^4\alpha_2^2-\alpha_1^2\alpha_2^4+\alpha_1^4\alpha_2^4}{\left(1+\alpha_1^2\right)^2\left(1+\alpha_2^2\right)^2\left(1-\alpha_1^2\alpha_2^2\right)}\cos 2k_F r\right] \\
&= 2\alpha_1\alpha_2\left(\frac{1}{k_F r}\right)^2\left[\frac{1+\alpha_1^4\alpha_2^4}{\left(1+\alpha_1^2\right)^2\left(1+\alpha_2^2\right)^2\left(1-\alpha_1^2\alpha_2^2\right)}(1-\cos 2k_F r)\right. \\
&\quad \left. +\frac{\alpha_1^2+\alpha_2^2+2\alpha_1^2\alpha_2^2+\alpha_1^4\alpha_2^2+\alpha_1^2\alpha_2^4}{\left(1+\alpha_1^2\right)^2\left(1+\alpha_2^2\right)^2\left(1-\alpha_1^2\alpha_2^2\right)}(1+\cos 2k_F r) + \frac{4\alpha_1^2\alpha_2^2}{\left(1+\alpha_1^2\right)^2\left(1+\alpha_2^2\right)^2\left(1-\alpha_1^2\alpha_2^2\right)}\cos 2k_F r\right] \\
&= 2\alpha_1\alpha_2\left(\frac{1}{k_F r}\right)^2\left[\frac{\left(1-\alpha_1^2\alpha_2^2\right)^2}{\left(1+\alpha_1^2\right)^2\left(1+\alpha_2^2\right)^2\left(1-\alpha_1^2\alpha_2^2\right)}(1-\cos 2k_F r)\right. \\
&\quad \left. +\frac{\alpha_1^2+\alpha_2^2+4\alpha_1^2\alpha_2^2+\alpha_1^4\alpha_2^2+\alpha_1^2\alpha_2^4}{\left(1+\alpha_1^2\right)^2\left(1+\alpha_2^2\right)^2\left(1-\alpha_1^2\alpha_2^2\right)}(1+\cos 2k_F r)\right] > 0
\end{aligned} \tag{A4}$$

because $\alpha_1,\alpha_2 < 1$. Analogously, when $\epsilon_1,\epsilon_2 < 0$,

$$\begin{aligned}
\frac{\delta\mathcal{E}}{\Delta_0} &= -\,2\alpha_1\alpha_2\left(\frac{1}{k_F r}\right)^2\left[\frac{\left(1-\alpha_1^2\alpha_2^2\right)^2}{\left(1+\alpha_1^2\right)^2\left(1+\alpha_2^2\right)^2\left(1-\alpha_1^2\alpha_2^2\right)}(1-\cos 2k_F r)\right. \\
&\quad \left. +\frac{\alpha_1^2+\alpha_2^2+4\alpha_1^2\alpha_2^2+\alpha_1^4\alpha_2^2+\alpha_1^2\alpha_2^4}{\left(1+\alpha_1^2\right)^2\left(1+\alpha_2^2\right)^2\left(1-\alpha_1^2\alpha_2^2\right)}(1+\cos 2k_F r)\right] > 0
\end{aligned} \tag{A5}$$

because $\alpha_1,\alpha_2 > 1$ so that the preferred magnetic orientation is antiferromagnetic when the energies are on the same side of the chemical potential. Now suppose $\epsilon_1, -\epsilon_2 > 0$, then we get

$$\begin{aligned}
\frac{\delta\mathcal{E}}{\Delta_0} &= 2\alpha_1\alpha_2\left(\frac{1}{k_F r}\right)^2\left[\frac{\alpha_1^2+\alpha_2^2+2\alpha_1^2\alpha_2^2+\alpha_1^4+\alpha_2^4+\alpha_1^4\alpha_2^2+\alpha_1^2\alpha_2^4}{\left(1+\alpha_1^2\right)^2\left(1+\alpha_2^2\right)^2\left(\alpha_1^2-\alpha_2^2\right)}\right. \\
&\quad \left. -\frac{\alpha_1^2+\alpha_2^2+6\alpha_1^2\alpha_2^2-\alpha_1^4-\alpha_2^4+\alpha_1^4\alpha_2^2+\alpha_1^2\alpha_2^4}{\left(1+\alpha_1^2\right)^2\left(1+\alpha_2^2\right)^2\left(\alpha_1^2-\alpha_2^2\right)}\cos 2k_F r\right] \\
&= 2\alpha_1\alpha_2\left(\frac{1}{k_F r}\right)^2\left[\frac{\alpha_1^2+\alpha_2^2+2\alpha_1^2\alpha_2^2+\alpha_1^4\alpha_2^2+\alpha_1^2\alpha_2^4}{\left(1+\alpha_1^2\right)^2\left(1+\alpha_2^2\right)^2\left(\alpha_1^2-\alpha_2^2\right)}(1-\cos 2k_F r)\right. \\
&\quad \left. +\frac{\alpha_1^4+\alpha_2^4}{\left(1+\alpha_1^2\right)^2\left(1+\alpha_2^2\right)^2\left(\alpha_1^2-\alpha_2^2\right)}(1+\cos 2k_F r) - \frac{4\alpha_1^2\alpha_2^2}{\left(1+\alpha_1^2\right)^2\left(1+\alpha_2^2\right)^2\left(\alpha_1^2-\alpha_2^2\right)}\cos 2k_F r\right] \\
&= 2\alpha_1\alpha_2\left(\frac{1}{k_F r}\right)^2\left[\frac{\alpha_1^2+\alpha_2^2+4\alpha_1^2\alpha_2^2+\alpha_1^4\alpha_2^2+\alpha_1^2\alpha_2^4}{\left(1+\alpha_1^2\right)^2\left(1+\alpha_2^2\right)^2\left(\alpha_1^2-\alpha_2^2\right)}(1-\cos 2k_F r)\right. \\
&\quad \left. +\frac{\left(\alpha_1^2-\alpha_2^2\right)^2}{\left(1+\alpha_1^2\right)^2\left(1+\alpha_2^2\right)^2\left(\alpha_1^2-\alpha_2^2\right)}(1+\cos 2k_F r)\right] < 0
\end{aligned} \tag{A6}$$

because $\alpha_2 > \alpha_1$. Therefore making a similar argument when $\epsilon_1 < 0$ and $\epsilon_2 > 0$, when the bare energies are on opposite sides of the chemical potential and sufficiently well separated, the impurities prefer to be oriented ferromagnetically.

In the special case when $\alpha_1 = \alpha_2 \equiv \alpha$, the energy levels diverge according to Eq. (A2). The expansion of the bound-state energies is instead given by

$$\begin{aligned}\epsilon_n(\theta) \approx{} & E_n + (-1)^n 4\alpha^2 \Delta_0 \frac{|\cos(\theta/2)|}{1+\alpha^2}\frac{\sin k_F r}{k_F r} \\ & + \alpha^2 \Delta_0 \left[2\alpha^2 \frac{1-(1-2\alpha^2)\cos 2k_F r}{(1-\alpha^2)^2(1+\alpha^2)^3} - \frac{1+\alpha^4-(1-4\alpha^2+\alpha^4)\cos 2k_F r}{(1-\alpha^2)^2(1+\alpha^2)^3}\cos\theta \right] \left(\frac{1}{k_F r}\right)^2 . \end{aligned} \tag{A7}$$

Although the leading order term contribution is of order $\exp(-r/\xi)/k_F r$ and oscillates with 2π periodicity in θ, the difference in total energy between the parallel and antiparallel configurations, when $\alpha < 1$ ($\alpha > 1$), again reduces to Eq. (A4) [Eq. (A5)] upon taking $\alpha_1, \alpha_2 \to \alpha$.

[1] L. Yu, Acta Phys. Sin. **21**, 75 (1965); H. Shiba, Prog. Theor. Phys. **40**, 435 (1968); A. I. Rusinov, Sov. Phys. JETP Lett. **9**, 85 (1969).

[2] A. Sakurai, Prog. Theor. Phys. **44**, 1472 (1970).

[3] A. Yazdani, B. A. Jones, C. P. Lutz, M. F. Crommie, and D. M. Eigler, Science **275**, 1767 (1997).

[4] M. E. Flatté and J. M. Byers, Phys. Rev. Lett. **78**, 3761 (1997).

[5] M. E. Flatté and J. M. Byers, Phys. Rev. B **56**, 11213 (1997).

[6] M. I. Salkola, A. V. Balatsky, and J. R. Schrieffer, Phys. Rev. B **55**, 12648 (1997).

[7] M. E. Flatté and J. M. Byers, Solid State Physics **52**, 137 (1999).

[8] M. E. Flatté and D. E. Reynolds, Phys. Rev. B **61**, 14810 (2000).

[9] A. V. Balatsky, I. Vekhter, and J.-X. Zhu, Rev. Mod. Phys. **78**, 373 (2006).

[10] S.-H. Ji, T. Zhang, Y.-S. Fu, X. Chen, X.-C. Ma, J. Li, W.-H. Duan, J.-F. Jia, and Q.-K. Xue, Phys. Rev. Lett. **100**, 226801 (2008).

[11] N. Y. Yao, L. I. Glazman, E. A. Demler, M. D. Lukin, and J. D. Sau, Phys. Rev. Lett. **113**, 087202 (2014).

[12] N. Y. Yao, C. P. Moca, I. Weymann, J. D. Sau, M. D. Lukin, E. A. Demler, and G. Zaránd, Phys. Rev. B **90**, 241108 (2014).

[13] A. A. Zyuzin and D. Loss, Phys. Rev. B **90**, 125443 (2014).

[14] T. Meng, J. Klinovaja, S. Hoffman, P. Simon, and D. Loss, Phys. Rev. B **92**, 064503 (2015).

[15] M. Ruby, F. Pientka, Y. Peng, F. von Oppen, B. W. Heinrich, and K. J. Franke, arXiv:1502.05048.

[16] S. Nadj-Perge, I. K. Drozdov, B. A. Bernevig, and A. Yazdani, Phys. Rev. B **88**, 020407 (2013).

[17] J. Klinovaja, P. Stano, A. Yazdani, and D. Loss, Phys. Rev. Lett. **111**, 186805 (2013).

[18] M. M. Vazifeh and M. Franz, Phys. Rev. Lett. **111**, 206802 (2013).

[19] B. Braunecker and P. Simon, Phys. Rev. Lett. **111**, 147202 (2013).

[20] S. Nakosai, Y. Tanaka, and N. Nagaosa, Phys. Rev. B **88**, 180503 (2013).

[21] F. Pientka, L. I. Glazman, and F. von Oppen, Phys. Rev. B **88**, 155420 (2013).

[22] K. Pöyhönen, A. Westström, J. Röntynen, and T. Ojanen, Phys. Rev. B **89**, 115109 (2014).

[23] I. Reis, D. J. J. Marchand, and M. Franz, Phys. Rev. B **90**, 085124 (2014).

[24] S. Nadj-Perge, I. K. Drozdov, J. Li, H. Chen, S. Jeon, J. Seo, A. H. MacDonald, B. A. Bernevig, and A. Yazdani, Science **346**, 602 (2014).

[25] R. Pawlak, M. Kisiel, J. Klinovaja, T. Meier, S. Kawai, T. Glatzel, D. Loss, and E. Meyer, arXiv:1505.06078.

[26] A. Heimes, P. Kotetes, and G. Schon, Phys. Rev. B **90**, 060507 (2014).

[27] P. M. R. Brydon, S. Das Sarma, Hoi-Yin Hui, and Jay D. Sau, Phys. Rev. B **91**, 064505 (2015).

[28] M. A. Ruderman and C. Kittel, Phys. Rev. **96**, 99 (1954); T. Kasuya, Prog. Theor. Phys. **16**, 45 (1956); K. Yosida, Phys. Rev. **106**, 893 (1957).

[29] P. Simon and D. Loss, Phys. Rev. Lett. **98**, 156401 (2007).

[30] B. Braunecker, P. Simon, and D. Loss, Phys. Rev. Lett. **102**, 116403 (2009).

[31] B. Braunecker, G. I. Japaridze, J. Klinovaja, and D. Loss, Phys. Rev. B **82**, 045127 (2010).

[32] T. Meng, P. Stano, J. Klinovaja, and D. Loss, Eur. Phys. J. B **87**, 203 (2014).

[33] P. W. Anderson and H. Suhl, Phys. Rev. **116**, 898 (1959).

[34] A. A. Abrikosov, *Fundamentals of the Theory of Metals*, Vol. 1 (Elsevier, Amsterdam, 1988).

[35] D. Aristov, S. Maleyev, and A. Yashenkin, Z. Phys. B **102**, 467 (1997).

[36] V. M. Galitski and A. I. Larkin, Phys. Rev. B **66**, 064526 (2002).

[37] A. I. Rusinov, Sov. Phys. JETP **29**, 1101 (1969); P. Schlottmann, Phys. Rev. B **13**, 1 (1976).

[38] D. K. Morr and J. Yoon, Phys. Rev. B **73**, 224511 (2006).

[39] In the case of $\alpha_1 = \alpha_2 = \alpha$, the expansion breaks down and the leading order contribution to the bound-state energy, which is valid when $|1-\alpha|k_F r \gg 1$, is $1/k_F r$. Upon summing the bound-state energies, the result coincides with $\mathcal{E}(\theta)$ taking $\alpha_1, \alpha_2 \to \alpha$. Therefore subject to the condition of weak hybridization, when the exchange interactions of the impurities are equal, antiferromagnetic orientation minimizes the energy (see Appendix).

[40] We note that the ferromagnetic and antiferromagnetic configurations in Fig. 3 are of different parity. As such, in the absence of quasiparticles [41–45], both configurations are ground states of the system in orthogonal Hilbert spaces with opposite parities. Pumping electrons into the bound states switches the parity of the system, for which one could probe flipping of the magnetic moment.

[41] P. J. de Visser, J. J. A. Baselmans, P. Diener, S. J. C. Yates, A. Endo, and T. M. Klapwijk, Phys. Rev. Lett. **106**, 167004 (2011).

[42] J. Aumentado, M. W. Keller, J. M. Martinis, and M. H. Devoret, Phys. Rev. Lett. **92**, 066802 (2004).

[43] D. Rainis and D. Loss, Phys. Rev. B **85**, 174533 (2012).
[44] D. J. van Woerkom, A. Geresdi, and L. P. Kouwenhoven, arXiv:1501.03855.
[45] A. P. Higginbotham, S. M. Albrecht, G. Kirsanskas, W. Chang, F. Kuemmeth, P. Krogstrup, T. S. Jespersen, J. Nygard, K. Flensberg, and C. M. Marcus, arXiv:1501.05155.
[46] R. Wiesendanger, Rev. Mod. Phys. **81**, 1495 (2009).
[47] M. S. Grinolds, S. Hong, P. Maletinsky, L. Luan, M. D. Lukin, R. L. Walsworth, and A. Yacoby, Nat. Phys. **9**, 215 (2013).
[48] P. Stano, J. Klinovaja, A. Yacoby, and D. Loss, Phys. Rev. B **88**, 045441 (2013).